Mechanical Systems and Signal Processing 42 (2014) 194–205

Contents lists available at ScienceDirect

Mechanical Systems and Signal Processing

journal homepage: www.elsevier.com/locate/ymssp

Autonomous dynamic displacement estimation from data fusion of acceleration and intermittent displacement measurements

Junhee Kim [a], Kiyoung Kim [b], Hoon Sohn [b,*]

[a] Department of Architectural Engineering, Dankook University, Jukjeon-ro 152, Suji-gu, Yongin-si, Gyunggi-do 448-701, Republic of Korea
[b] Department of Civil and Environmental Engineering, Korea Advanced Institute of Science and Technology, Daejeon 305-701, Republic of Korea

ARTICLE INFO

Article history:
Received 20 March 2013
Received in revised form
8 September 2013
Accepted 25 September 2013
Available online 10 October 2013

Keywords:
Structural measurement
Displacement estimation
Acceleration integration
Sensor data fusion
Multi-rate Kalman filtering

ABSTRACT

Addressing the importance of displacement measurement of structural responses in the field of structural health monitoring, this paper presents an autonomous algorithm for dynamic displacement estimation from acceleration integration fused with displacement data intermittently measured. The presented acceleration integration algorithm of multi-rate Kalman filtering distinguishes itself from the past study in the literature by explicitly considering acceleration measurement bias. Furthermore, the algorithm is formulated by unique state definition of integration errors and error dynamics system modeling. To showcase performance of the algorithm, a series of laboratory dynamic experiments for measuring structural responses of acceleration and displacement are conducted. Improved results are demonstrated through comparison between the proposed and past study.

1. Introduction

Traditionally displacement response of structures has provided useful information to the field of structural engineering, since it can be directly converted to deformation and strain of the structures [1]. Besides the traditional preference, there are strong needs for measurement of displacement in the recent fields of health monitoring, safety/condition assessment, and system identification for civil engineering structures: for example, based on measured static and pseudo-static deflections of a bridge deck for heavy duty trucks, bridge load carrying capacity can be determined; dynamic displacement measurement are preferred over acceleration measurement in the context of system identification, since the use of displacement data as system output results in a state-space model which can be converted to physically interpretable parameters [2,3].

In practice, displacement response measurement of existing structures is fairly difficult and cumbersome. Since displacement is a relative physical quantity, it requires a reference. Thus, contact displacement sensors (e.g., LVDT and potentiometer) require stationary platforms which may increase installation cost and deteriorate accuracy of measurements. Being proposed as the alternatives, non-contact optical technology (e.g., laser scanning instruments [4]) and computer vision-based [5] and GPS-based technology [6] are popular these days. However, the relating problems still remain unsolved such as high equipment cost, low sampling rate, low resolution, just to name a few.

* Corresponding author. Tel.: +82 42 350 3665.
E-mail address: hoonsohn@kaist.ac.kr (H. Sohn).

0888-3270/$ - see front matter © 2013 Elsevier Ltd. All rights reserved.
http://dx.doi.org/10.1016/j.ymssp.2013.09.014

There has been a strong preference of the use of measured acceleration to retrieve displacement (which is equivalent with physical quantities of position and location), since acceleration can be easily measured without a fixed reference point in the numerous fields of science and engineering (e.g., structural engineering, seismology, geodetic and navigation). Direct integration of measured acceleration yields displacement mathematically. However, the simple integration of acceleration suffers from drift issue. A plethora of strategies for remedies against case-by-case drift problems have been actively studied especially in the field of engineering seismology and are mainly categorized into two groups: baseline correction and low and high pass filtering [7]. Baseline correction is a least-square curve fitting technique in the time domain and filtering is a common noise removal technique in the frequency domain. As for displacement estimation of dynamic and pseudo-static displacements of bridge girders under passing traffic, Park et al. (2005) proposed an iterative methodology termed as the initial velocity estimation method (IVEM) by single integration of estimated velocity time histories with a zero initial value [8]. More recently, use of an analytical state-space model was proposed to correct displacement estimates of dynamic response of a bridge under vehicular load [9].

In general, it is accepted that a universal correction scheme which can be autonomously applied to pure acceleration integration is rather challenging to yield satisfactory results [10]. Thus, it seems to be inevitable to combine acceleration and intermittently measured displacement. Utilizing fusion of inherent data redundancy, high accurate displacement and velocity are estimated. The multi-rate Kalman filtering technique has been actively applied to the data fusion especially in the field of navigation and guidance [11,12]. The most significant merit of Kalman filtering is its autonomous implementation without any need of human involvement and judge unlike the aforementioned correction scheme for acceleration integration. In this context, data fusion by Kalman and its variant filtering (i.e., unscented Kalman filtering, particle filtering, etc.) has been emerged as an active research stream in the SHM community: Smyth and Wu presented a multi-rate Kalman filtering algorithm for the purpose of estimating dynamic displacement from acceleration and intermittent displacement measurements with various numerical examples [13]; Chang and Xiao applied it to an experimental example of acceleration and videogrammetric displacement sensing [14]; addressing the limit of a constant noise variance of Kalman filtering, Li and Chang proposed an adaptive time-varying noise estimation algorithm by virtue of signal subspace tracking [15].

In this study, a new algorithm of the multi-rate Kalman filtering is presented for improving accuracy of dynamic displacement estimation based on continuous acceleration and intermittent displacement measurements. The proposed estimation algorithm explicitly considers acceleration measurement bias to reflect the accelerometer inherent bias during acceleration integration. In order to consider the acceleration measurement bias, integration error evolution is modeled as system dynamics of Kalman filtering. Detailed derivation and implementation of the error dynamics-based Kalman filtering is discussed theoretically. Experimental verification is then followed using data sets of acceleration and displacement sensed by a laser optic sensor.

2. Displacement estimation from acceleration integration

2.1. Problem statement of acceleration integration

Single and double successive numerical integrations of the measured acceleration of an object in the discrete-time domain with the time interval, Δt, calculate velocity and displacement respectively as

$$\dot{x}(k+1) = \dot{x}(k) + \ddot{x}(k)\Delta t \tag{1}$$

$$x(k+1) = x(k) + \dot{x}(k)\Delta t + 0.5\ddot{x}(k)\Delta t^2 \tag{2}$$

where $\dot{x}(k)$ and $x(k)$ are the calculated velocity and displacement at the time step k, $\ddot{x}(k)$ is the measured acceleration at the time step k. Two inherent problems relating with the acceleration integration can be addressed. Seen in Eqs. (1) and (2), numerical error can be accumulated due to the zero-order hold (i.e., the values at the time step of $k+1$ are calculated from the fixed values at the time step k) and referred to as mathematical error. This is inevitable to deal with continuous-time physical phenomena in the discrete-time domain. Furthermore, there is a more fundamental problem that Eqs. (1) and (2) are based on the measured acceleration different from the true acceleration.

The measured acceleration is contaminated by measurement error and thus written in the discrete-time domain as

$$\ddot{x}(k) = \bar{\ddot{x}}(k) + \varepsilon\ddot{x}(k) \tag{3}$$

where $\bar{\ddot{x}}(k)$ is the true acceleration at the time step k, and $\varepsilon\ddot{x}(k)$ is the acceleration measurement error at the time step k. Therefore, the problem of estimating displacement and velocity from integration of the measured acceleration can be converted to that of estimating the acceleration measurement error, $\varepsilon\ddot{x}(k)$ and its contribution to integration errors. Based on the estimated error, the numerical integration can be compensated and the estimates of velocity and displacement, $\hat{\dot{x}}$ and $\hat{x}$, are calculated respectively as

$$\hat{\dot{x}}(k+1) = \hat{\dot{x}}(k) + \ddot{x}(k)\Delta t - \varepsilon\ddot{x}(k)\Delta t \tag{4}$$

$$\hat{x}(k+1) = \hat{x}(k) + \hat{\dot{x}}(k)\Delta t + 0.5\ddot{x}(k)\Delta t^2 - 0.5\varepsilon\ddot{x}(k)\Delta t^2 \tag{5}$$

2.2. Multi-rate Kalman filtering for integration error estimation

The acceleration measurement error, $\varepsilon\ddot{x}(k)$, can be considered a combination of offset bias, $b(k)$ (e.g., mechanical or electrical hysteresis [7] and accelerometer installation errors including inaccurate alignment) and zero-mean stochastic noise process, $w(k)$

$$\varepsilon\ddot{x}(k) = b(k) + w(k) \tag{6}$$

The stochastic noise process is assumed as stationary zero-mean Gaussian process (i.e., $w(k)$–$N(0,q)$) and does not significantly deteriorate the numerical integration (i.e., Eqs. (1) and (2)) due to the nature of zero-mean. However, the offset bias could significantly induce the drift problem during the successive numerical integration.

In order to estimate the acceleration measurement error and to compensate the numerical integration, the multi-rate Kalman filtering for data fusion of acceleration and displacement measured is adopted in this study. State variables for the continuous-time state-space model of Kalman filter are introduced as acceleration error (i.e., bias) and its single and double integrations (i.e., velocity and displacement integration errors), respectively:

$$\mathbf{x}(t) = [\varepsilon x(t)\ \varepsilon\dot{x}(t)\ \ b(t)]^T \tag{7}$$

where $\varepsilon x(t)$ is the displacement integration error and $\varepsilon\dot{x}(t)$ is the velocity integration error. Considering a differential operator (i.e., a matrix of unit elements at upper-diagonals), a state-space model can be formulated in the continuous-time domain as

$$\dot{\mathbf{x}}(t) = \begin{bmatrix} 0 & 1 & 0 \\ 0 & 0 & 1 \\ 0 & 0 & 0 \end{bmatrix} \mathbf{x}(t) + \begin{bmatrix} 0 \\ 1 \\ 0 \end{bmatrix} w(t) = \mathbf{A}\mathbf{x}(t) + \mathbf{B}w(t) \tag{8}$$

It should be noted that the equation for the state variable of b is $\dot{b}(t) = 0$ in Eq. (8) and implies that the acceleration measurement bias remains constant during time update stage. However, it will be updated at correction stage later (as defined as a time-variant state variable in Eq. (7)). The continuous-time model can be converted to the discrete-time model with the time interval Δt as

$$\mathbf{x}(k+1) = \mathbf{A}_d\mathbf{x}(k) + \mathbf{B}_\mathrm{d}w(k) \tag{9}$$

where the discrete-time system matrix, $\mathbf{A}_\mathrm{d}$ and noise process vector, $\mathbf{B}_\mathrm{d}$ are calculated from the fact that $\mathbf{A}$ is nilpotent (i.e.,$\mathbf{A}^3 = \mathbf{0}$) respectively as

$$\mathbf{A}_d = e^{\mathbf{A}\Delta t} = \mathbf{I} + \mathbf{A}\Delta t + \frac{\mathbf{A}^2}{2!}\Delta t^2 = \begin{bmatrix} 1 & \Delta t & 0.5\Delta t^2 \\ 0 & 1 & \Delta t \\ 0 & 0 & 1 \end{bmatrix} \tag{10}$$

$$\mathbf{B}_d = \left(\int_0^{\Delta t} e^{\mathbf{A}\tau} d\tau\right)\mathbf{B} = \left(\mathbf{I}\Delta t + \frac{1}{2!}\mathbf{A}\Delta t^2 + \frac{1}{3!}\mathbf{A}^2\Delta t^3\right)\mathbf{B} = \begin{bmatrix} 0.5\Delta t^2 \\ \Delta t \\ 0 \end{bmatrix} \tag{11}$$

Then, a priori state estimate for the error evolution is calculated as

$$\mathbf{x}(k+1|k) = \mathbf{A}_d\mathbf{x}(k|k) \tag{12}$$

A priori state covariance for the error evolution is also expressed as

$$\mathbf{P}(k+1|k) = \mathbf{A}_d\mathbf{P}(k|k)\mathbf{A}_\mathrm{d}^\mathrm{T} + \mathbf{Q}_\mathrm{d} \tag{13}$$

where the discrete-time stochastic noise covariance matrix, $\mathbf{Q}_\mathrm{d}$ is determined with the given variance of the stationary Gaussian process (i.e., $N(0,q)$) and the derived discrete-time noise process vector in Eq. (11) as

$$\mathbf{Q}_\mathrm{d} = q\mathbf{B}_\mathrm{d}\mathbf{B}_\mathrm{d}^\mathrm{T} = q\begin{bmatrix} \Delta t^4/4 & \Delta t^3/2 & 0 \\ \Delta t^3/2 & \Delta t^2 & 0 \\ 0 & 0 & 0 \end{bmatrix} \tag{14}$$

Eqs. (12) and (13) are considered the time update of the multi-rate Kalman filtering (i.e., prediction). Based on the estimated a priori state variables for velocity error and displacement error (i.e., $\varepsilon\dot{x}(k+1|k)$ and $\varepsilon x(k+1|k)$), the calculated velocity and displacement (i.e., $\dot{x}(k+1)$ and $x(k+1)$ by the numerical integrations of Eqs. (1) and (2), respectively) are compensated as

$$\hat{\dot{x}}(k+1|k) = \dot{x}(k+1) - \varepsilon\dot{x}(k+1|k) \tag{15}$$

$$\hat{x}(k+1|k) = x(k+1) - \varepsilon x(k+1|k) \tag{16}$$

The measurement update of the multi-rate Kalman filtering (i.e., correction) is conducted when displacement data is collected. Assuming displacement data is acquired at the time step j, displacement error can be calculated by the difference

between the measured displacement, $x_{disp}(j)$ and calculated displacement, $x(j)$based on the numerical integration of Eq. (2)

$$y(j) = x(j) - x_{disp}(j) \tag{17}$$

where $y(j)$ is the calculated displacement error. Displacement error can be also acquired from observation of the state variables. This can be considered observation of the estimated a priori state of the displacement error, $\varepsilon x(j)$ and written as an observation equation:

$$z(j) = \mathbf{C}_d \mathbf{x}(j|j-1) + v(j) \tag{18}$$

where $z(j)$ is the observed displacement error, the observation matrix is $\mathbf{C}_d = [1 \quad 0 \quad 0]$, and $v(j)$ is the uncertainty relating to observation of the displacement error. In this study, the uncertainty is assumed as being stationary zero-mean Gaussian (i.e., $v(j)$–$N(0,r)$) and treated by that of the displacement measurement. Thus, a posteriori state estimate and state covariance for error evolution are calculated, respectively, as [16]

$$\mathbf{x}(j|j) = \mathbf{x}(j|j-1) + \mathbf{K}(j)(y(j) - \mathbf{C}_d \mathbf{x}(j|j-1)) \tag{19}$$

$$\mathbf{P}(j|j) = (\mathbf{I} - \mathbf{K}(j)\mathbf{C}_d)\mathbf{P}(j|j-1) \tag{20}$$

where Kalman gain, $\mathbf{K}(j)$ is calculated as

$$\mathbf{K}(j) = \mathbf{P}(j|j-1)\mathbf{C}_d^T(\mathbf{C}_d\mathbf{P}(j|j-1)\mathbf{C}_d^T + r)^{-1} \tag{21}$$

Based on the a posteriori state estimates of velocity and displacement errors (i.e., $\varepsilon\dot{x}(j|j)$ and $\varepsilon x(j|j)$), the calculated velocity and displacement (i.e., $\dot{x}(j)$ and $x(j)$) by the numerical integrations are compensated as

$$\hat{\dot{x}}(j|j) = \dot{x}(j) - \varepsilon\dot{x}(j|j) \tag{22}$$

$$\hat{x}(j|j) = x(j) - \varepsilon x(j|j) \tag{23}$$

In summary, Fig. 1 illustrates the aforementioned mulit-rate Kalman filtering for estimation of integration error evolution conceptually.

2.3. Optimal smoothing for enhancement of Kalman filtering

Displacement estimated by the aforementioned multi-rate Kalman filtering might still suffer from drift problem when dealing with a large interval of displacement updates and significant acceleration measurement errors. Optimal smoothing can be adopted to enhance the accuracy of the multi-rate Kalman filtering. Unlike on-line real-time implementation of Kalman filtering, fixed-interval smoothing can be implemented off-line with complete time histories of the measured data. Namely, the aforementioned Kalman filtering is implemented forward and backward in time. The fixed interval smoothing then combines the results of the forward and backward Kalman filtering. The entire implementation of the backward Kalman filtering is identical with that of the forward Kalman filtering described in Section 2.2 except the use of a negative time interval, Δt.

Let us assume that we complete the forward and backward Kalman filtering: two displacement estimates (i.e., $\hat{x}_f(k)$and$\hat{x}_b(k)$) and covariances (i.e., $P_f(k)$ and $P_b(k)$) are calculated in the whole time line. The smoothed displacement estimate, $\hat{x}_s(k)$ can be calculated as

$$\hat{x}_s(k) = K_f(k)\hat{x}_f(k) + K_b(k)\hat{x}_b(k) \tag{24}$$

where $K_f(k)$ and $K_b(k)$ are coefficients that weigh the relative contribution of the forward and backward estimates. To guarantee an unbiased displacement estimate, it requires that the sum of the two coefficients equals one. Thus, Eq. (23) can be written as

$$\hat{x}_s(k) = K_f(k)\hat{x}_f(k) + (1 - K_f(k))\hat{x}_b(k) \tag{25}$$

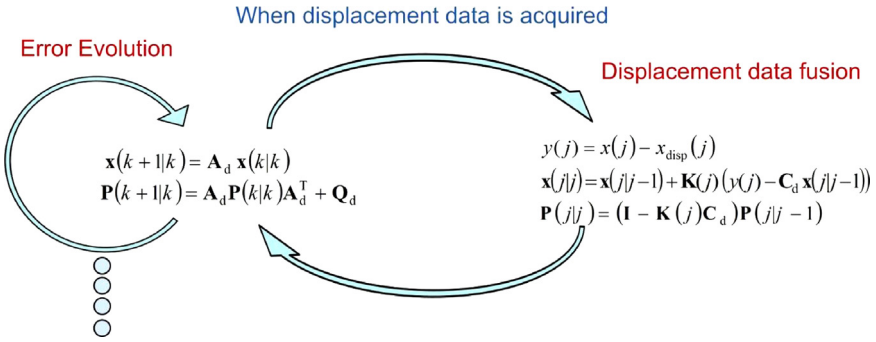

Fig. 1. Integration error evolution and correction by displacement data fusion.

Definition of the covariance of the smoothed estimate (i.e., $P_s(k) = \mathrm{cov}(\hat{x}_s(k)\ \hat{x}_s(k))$) leads to

$$P_s(k) = K_f(k)P_f(k)K_f(k) + (1-K_f(k))P_b(k)(1-K_f(k)) \tag{26}$$

Minimizing $P_s(k)$ of Eq. (25) with respect to $K_f(k)$ (i.e., $\partial P_s/\partial K_f = 0$) yields the optimal coefficient of $K_f(k)$ as

$$K_f(k) = P_b(k)(P_f(k)+P_b(k))^{-1} \tag{27}$$

By substituting the optimal coefficient into Eqs. (24) and (25), the smoothed displacement and its covariance can be determined, respectively, as

$$\hat{x}_s(k) = P_b(k)(P_f(k)+P_b(k))^{-1}\hat{x}_f(k) + P_f(k)(P_f(k)+P_b(k))^{-1}\hat{x}_b(k) \tag{28}$$

$$P_s(k) = (P_f^{-1}(k)+P_b^{-1}(k))^{-1} \tag{29}$$

Identical approach can be applied to calculate the smoothed velocity and bias estimates.

3. Experimental application

Performance of the multi-rate Kalman filtering and smoothing for displacement and velocity estimates is evaluated with experimentally collected data. Based on data fusion of continuous acceleration and intermittent displacement measurements, dynamic displacement and velocity can be estimated by the proposed algorithm. However, in order to quantitatively evaluate displacement estimates, continuous displacement measurement by laser Doppler vibrometer (LDV) is adopted in the experimental phase of this study, since the displacement measured can be a reference.

3.1. Experimental setup

A small scaled cantilever beam is built with a steel strip of 40 cm × 2 cm × 2 mm. The structural response of the beam is measured at a single point of the free end simultaneously by two transducers: piezoelectric accelerometer (353B15, PCB Piezotronics) and LDV (PSV-400-M4, Polytec GmbH). Unlike the accelerometer mounted on one side of the beam, the LDV is placed about one meter away from the cantilever beam aiming its laser beam at the center point of the accelerometer. The LDV is a precision optical transducer to determine dynamic displacement by sensing the frequency shift of back scattered light from a moving surface. The experimental setup is depicted in Fig. 2.

3.2. Experimental data processing

Since the purpose of the experiment is to collect data set of displacement and acceleration at a specific point of the beam in dynamic motion, simple excitation methods are adopted: finger-tapping on the surface of the beam (termed Case I); impacting by a small modal hammer (PCB Piezotronics 086C03) (termed Case II); non-oscillatory manual excitation to mimic pseudo-static behavior of the beam (termed Case III). For each case, 20 s displacement and acceleration data set is collected with the sampling time of 0.655 ms. It should be noted that additional descriptions on characteristics of excitation signal, structural natural frequencies, and selection of the sampling time are not necessary, since the proposed multi-rate Kalman filtering can be implemented autonomously. The only parameter which affects accuracy of the filtering is the displacement sampling rate with respect to the continuous acceleration measurement (i.e., update rate); obviously, the accuracy of the filtering improves as the displacement sampling rate increases. Relatively low displacement sampling rate is set as 50 (i.e., 50×0.655 ms $= 0.03275$ s update time interval) so as to investigate performance of the proposed method. However, effects of various sampling rates to the accuracy will be also explored later (Fig. 3).

Since the structural response of Case I (i.e., arbitrary finger-tapping excitation) has a wide range of frequency components, it is selected as an example discussed in detail. Fig. 4 displays results of forward implementation of the multi-rate Kalman filtering using the data set of Case I. Overall, a close agreement between the displacement estimates and the reference displacements measured by the LDV is observed over the whole time line of 0 to 20 s (Fig. 4(a)). However, slightly overestimated displacements are also found occasionally. A close up of Fig. 4(a) is presented in Fig. 4(b) for the purpose of a detailed investigation of displacement estimates: in the time range of 10–10.7 s, the estimates follow the reference without any significant drift at every update time step. The small differences between a priori and a posteriori displacement estimates result from accurate acceleration measurements. Relatively significant drifts from the reference are found in the time range of 10.7 –11 s. The velocity and accelerometer bias estimates are also presented in Fig. 4(c) and (d), respectively: the accelerometer bias estimates quickly converge to -0.046 m/s^2 after a strong initial fluctuation. The uncertainties relating to the three estimates (i.e., variances of displacement, velocity, and accelerometer bias estimates) are depicted in Fig. 4(e): fast convergences from the initial set of 1 to trivial levels in which the variances fluctuate repeatedly are observed.

Similar tendencies are also found in the results of backward implementation of the multi-rate Kalman filtering using the data set of Case I as depicted in Fig. 5. The reason of non-identical results between the forward and backward filtering can be explained by the quadratic terms in the filtering equations (e.g., the time interval in Eq. (10) and Kalman gain). Enhanced estimates smoothed by the forward and backward Kalman filtering are observed in Fig. 6: excellent agreement between the

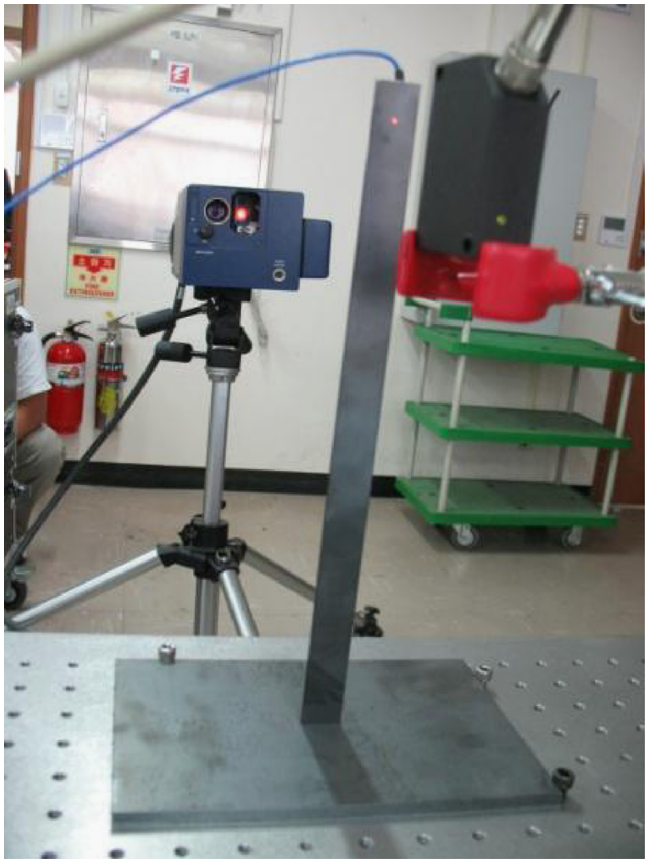

Fig. 2. Experimental setup: collocated measurement of acceleration and displacement at a cantilever beam.

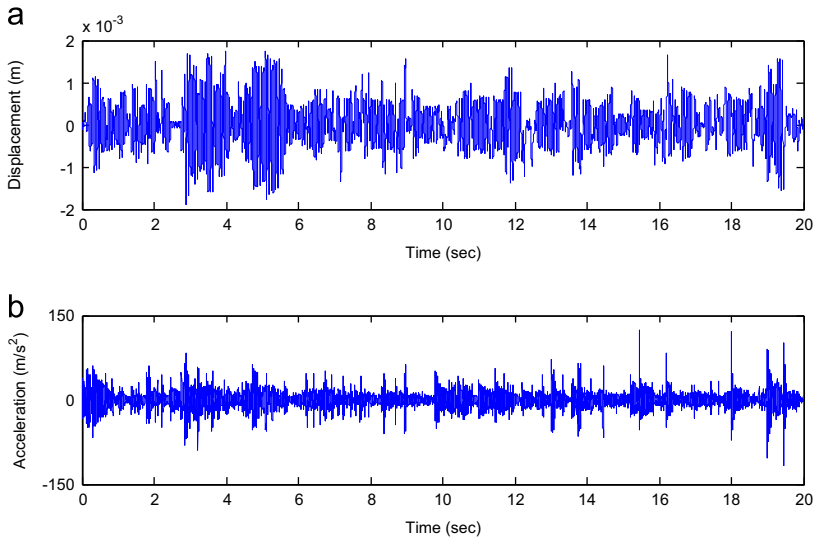

Fig. 3. Case I: (a) measured displacement and (b) measured acceleration.

estimates and reference is seen through the whole time line (Fig. 6(a) and (b)); a consistent negative acceleration bias (i.e., -0.046 m/s^2) is also found in Fig. 6(c).

Satisfactory displacement estimates at the other two excitation cases such as Case II (i.e., impact excitation) and Case II (i.e., non-oscillatory excitation) are also verified. For the purpose of presenting legible figures, only initial 5 s measured data and estimate results are depicted in Figs. 7 and 8 respectively for Case II and Case III. The repeated notable discrepancies

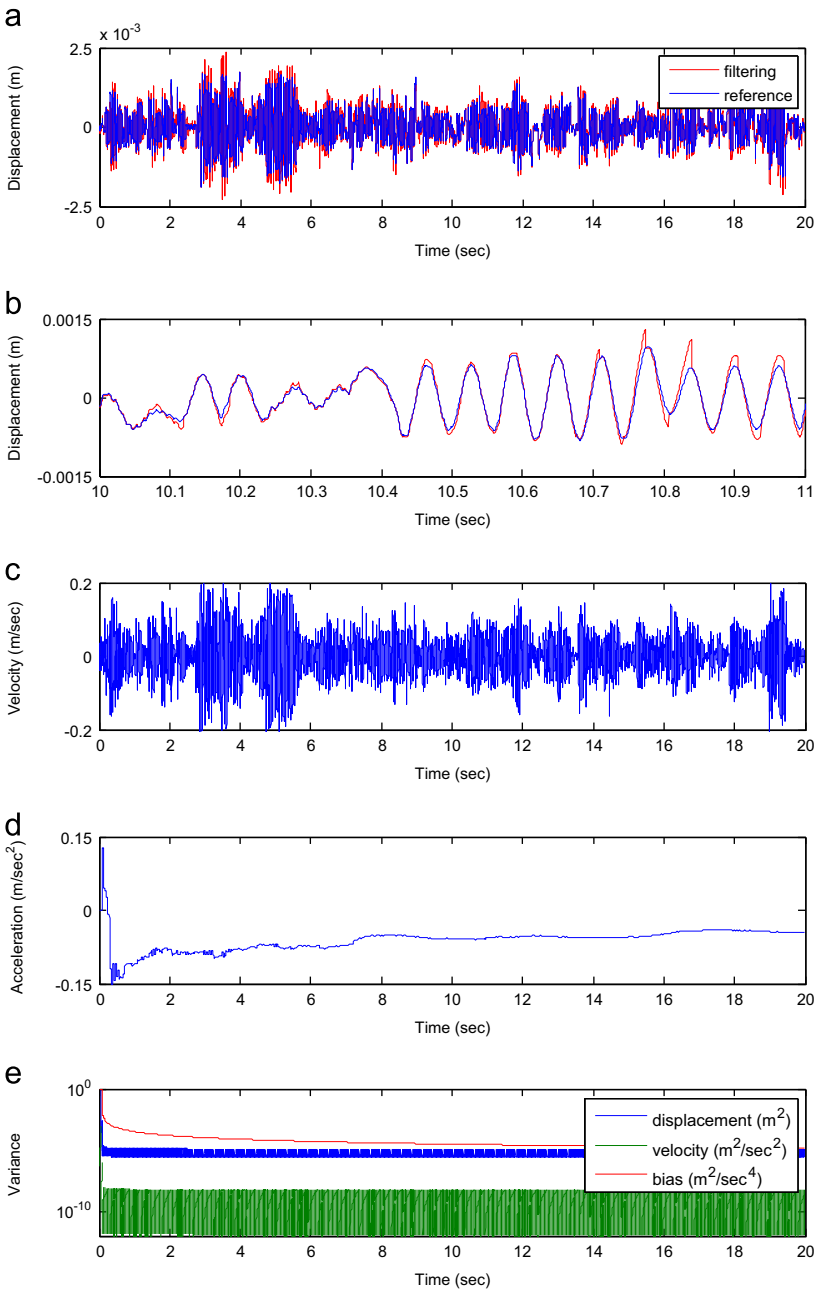

Fig. 4. Forward multi-rate Kalman filtering with the displacement sampling rate of 50 (Case I): (a) measured displacement (i.e., reference), $x_{\text{disp}}(j)$ and displacement estimate, $\hat{x}(k+1|k)$ or $\hat{x}(k+1|k+1)$; (b) close-up of (a) for 10–11 s; (c) velocity estimate, $\hat{x}(k+1|k)$ or $\hat{x}(k+1|k+1)$; (d) acceleration measurement bias estimate, $b(k)$; and (e) variances for displacement error, velocity error, and acceleration bias, $\mathbf{P}(k+1|k)$ or $\mathbf{P}(k+1|k+1)$.

between the reference and estimate are observed at peaks along free vibration response in Fig. 7(b), which can be explained by time interval proximity between the displacement update time (i.e., 0.03275 s) and half of the first natural period of the beam (i.e., 0.03113 s).

A quantitative performance evaluation of the proposed algorithm is conducted by calculating RMS errors between the displacement estimates and reference (i.e., $\sqrt{\sum(\hat{x}(k)-x_{\text{disp}}(k))^2/N}$, N=number of data). As a result, RMS errors calculated with the aforementioned filtering and smoothing for the three cases are tabulated in Table 1. As seen, comparable accuracies are found between the results of forward and backward Kalman filtering but significantly increased accuracies are consistently found in smoothing through the three cases.

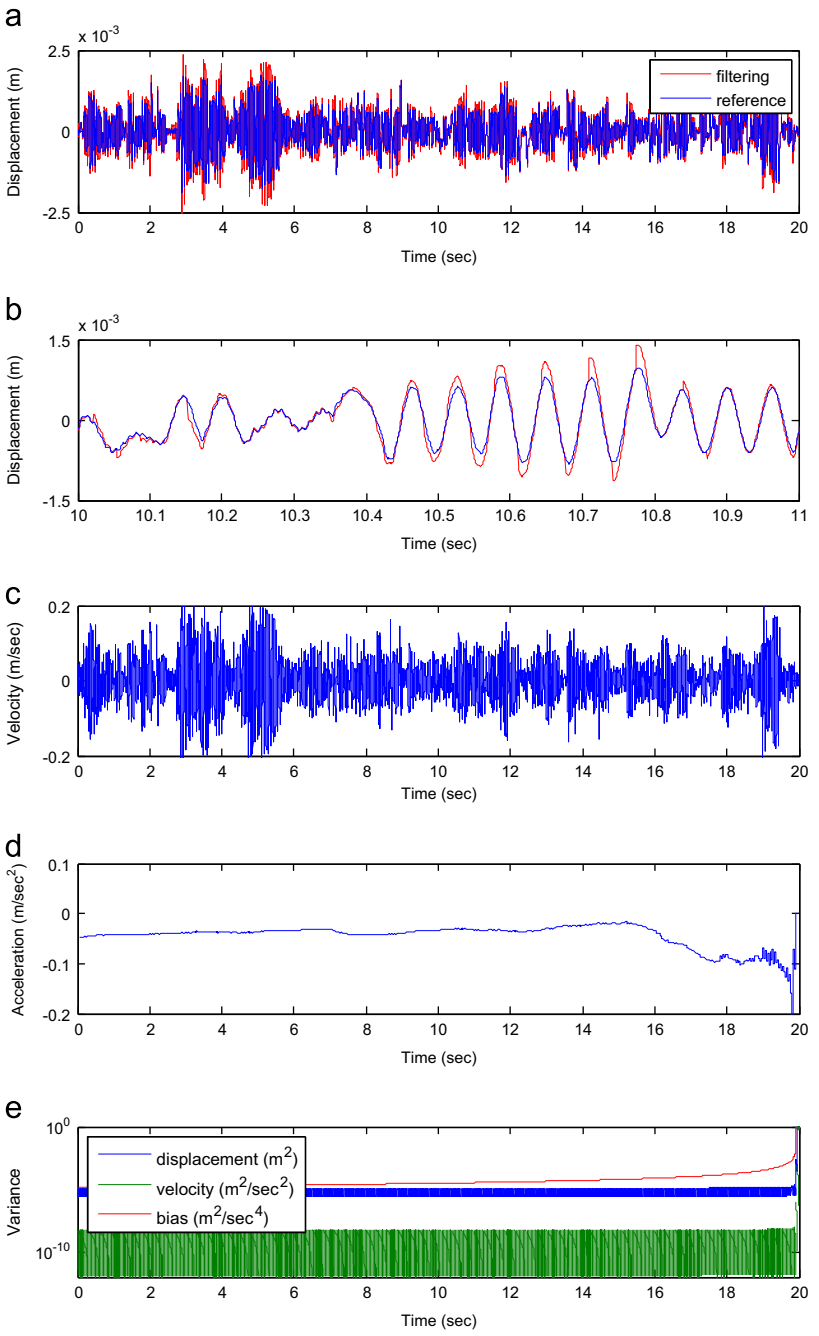

Fig. 5. Backward multi-rate Kalman filtering with the displacement sampling rate of 50 (Case I): (a) measured displacement (i.e., reference), $x_{\text{disp}}(j)$ and displacement estimate, $\hat{x}(k+1|k)$ or $\hat{x}(k+1|k+1)$; (b) close-up of (a) for 10–11 s; (c) velocity estimate, $\hat{x}(k+1|k)$ or $\hat{x}(k+1|k+1)$; (d) acceleration measurement bias estimate, $b(k)$; and (e) variances for displacement error, velocity error, and acceleration bias, $\mathbf{P}(k+1|k)$ or $\mathbf{P}(k+1|k+1)$.

In order to explore benefits of explicit formulation of acceleration measurement bias and integration error compensation proposed by this study, a comparison study with the algorithm proposed by Smyth and Wu (2007) is conducted: the identical data sets of the three cases are processed by the algorithm to estimate displacements. Comparison study is confined only to forward Kalman filtering and the corresponding RMS errors are inserted in Table 1 with their ratios (i.e., A/B). Improved accuracies (i.e., less RMS errors) are verified at the proposed algorithm compared to that of Smyth and Wu's algorithm: slightly improved estimate results are found at Cases I and II which are the cases of acceleration measurements for oscillatory motions of the beam. However, relatively significant improvement is found at Case III of acceleration measurements for non-oscillatory pseudo-static motion of the beam. The observation can be explained by the fact that repeated state estimations both at the increasing and decreasing tendency (as illustrated at Fig. 4(b)) alleviate accumulation

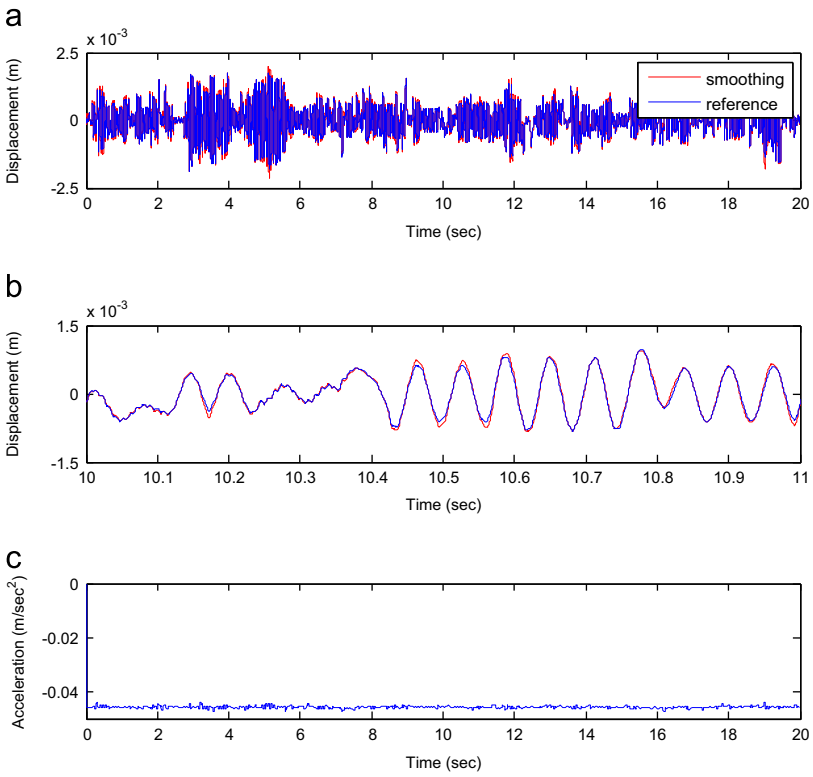

Fig. 6. Smoothing with the displacement sampling rate of 50 (Case I): (a) measured displacement (reference) and displacement estimate; (b) close-up of (a) for 10 to 11 s; and (c) acceleration measurement bias estimate.

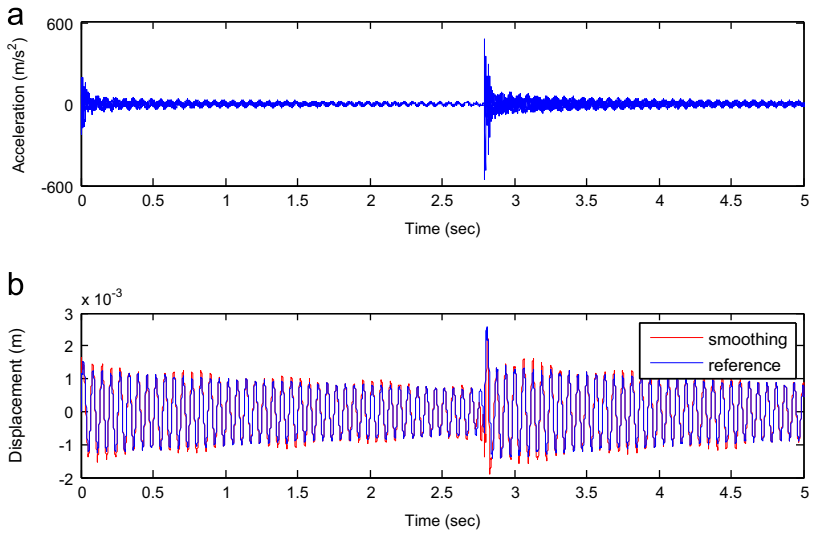

Fig. 7. Case II: (a) measured acceleration and (b) measured displacement (reference) and displacement estimate by smoothing with the displacement sampling rate of 50.

of the acceleration measurement bias in the case of oscillatory motions (i.e., vibrations); in the case of non-oscillatory motion, accumulation of acceleration measurement bias significantly affects the accuracy of displacement estimates by the acceleration integration. Improved performance of the proposed algorithm over that of Smyth and Wu's is depicted in Fig. 9. Two notable aspects of the displacement estimates by the proposed algorithm can be found: (1) smaller drift happens during the prediction stage of Kalman filtering due to consideration of the acceleration measurement bias and (2) closer a posteriori estimates (i.e., much less offset compared to that from Smyth and Wu's) are calculated at the correction stage of Kalman filtering thanks to the error dynamics formulation.

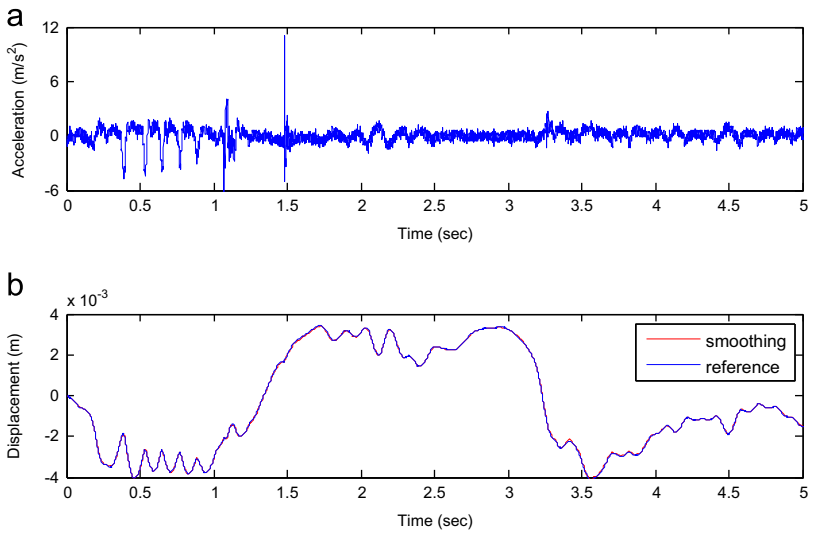

Fig. 8. Case III: (a) measured acceleration and (b) measured displacement (reference) and displacement estimate by smoothing with the displacement sampling rate of 50.

Table 1
RMS errors of displacement estimates from filtering and smoothing for displacement sampling rates of 50 (unit: m).

	Forward Kalman filtering			Backward Kalman filtering	Smoothing
	Proposed (A)	Smyth & Wu (B)	A/B (%)		
Case I	1.36E−04	1.41E−04	96.74	1.58E−04	6.81E−05
Case II	4.58E−04	4.70E−04	97.35	4.94E−04	1.86E−04
Case III	4.43E−05	5.13E−05	86.30	4.51E−05	1.77E−05

Effect of displacement sampling rates to smoothing estimates is explored and summarized in Table 2 with RMS errors of the estimate and reference. An intuitive conclusion can be drawn: as the displacement sampling rate increases (i.e., the frequency of displacement measurement update becomes slower), the accuracy of displacement estimate is deteriorated. However, the RMS error at the displacement sampling rate of 100 (i.e., at most 385.5% of that of the displacement sampling rate of 50) implies the proposed smoothing algorithm for displacement estimates still works acceptably even in the worst case.

4. Conclusions

This paper presents a novel multi-rate Kalman filtering for dynamic displacement estimation from the data fusion of continuous acceleration and intermittent displacement measurements. Based on explicit consideration of acceleration measurement bias, integration error evolution is modeled as system dynamics in Kalman filtering. Excellent performance of the proposed method is verified through experimental data of three different types of structural responses: arbitrary vibration, free vibration, and non-oscillatory pseudo-static motion. Based on data processing with the experimental data, it is confirmed that the proposed method yields displacement estimates with improved accuracy compared to reference in the literature.

Numerous applications of the autonomous data fusion approach are expected for processing heterogeneous and multi-rate measurement data – e.g., combination of acceleration and displacement sensed by GPS and video camera. In addition to accurate displacement estimation, velocity estimate can be also utilized for monitoring the structures in dynamic motion. Furthermore, the data fusion strategy of estimating displacement can be extended to estimate rotational variables by measuring linear variables (i.e., acceleration and displacement) at two different points and constituting a geometric equation for relationship between the linear and rotational variables.

Acknowledgment

This work is supported by the Leap Research Program (2010-0017456) of the National Research Foundation (NRF) of Korea funded by Ministry of Education, Science and Technology (MEST) and Grant (12CCTI-C063754-01) from Construction

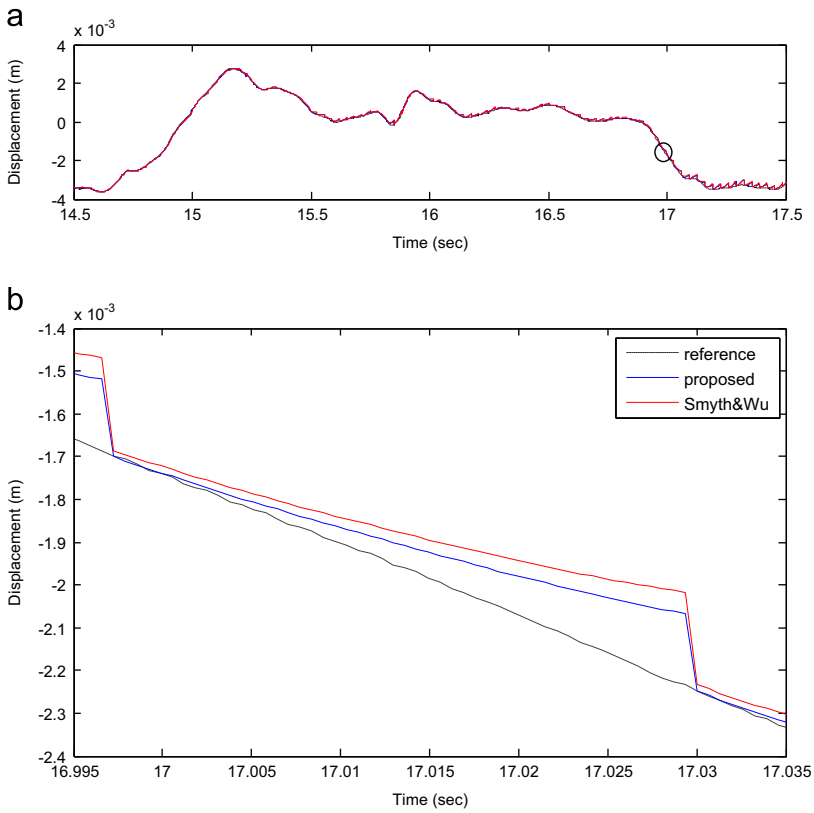

Fig. 9. Performance comparison between algorithms proposed and of Smyth and Wu (2007) for forward Kalman filtering implementation with the displacement sampling rate of 50: (a) displacement estimates during the time interval of 14.5–17.5 s for Case III; (b) a typical single cycle of Kalman filtering (i.e., close-up of estimates denoted as a circle in (a)).

Table 2
Summary of RMS errors of displacement estimates from smoothing for various displacement sampling rates (unit: m): the numbers in the parenthesis are ratio of RMS errors of the case to that of the displacement sampling rate of 50.

	Displacement sampling rates			
	10	20	50	100
Case I	6.52E−06 (9.6%)	1.30E−05 (19.1%)	6.81E−05	1.03E−04 (151.6%)
Case II	1.85E−05 (9.9%)	3.96E−05 (21.3%)	1.86E−04	5.35E−04 (287.2%)
Case III	3.12E−06 (17.7%)	4.32E−06 (24.5%)	1.77E−05	6.80E−05 (385.5%)

Technology Innovation Program funded by Ministry of Land, Transport and Maritime Affairs (MLTM) of Korea Government and Korea Institute of Construction & Transportation Technology Evaluation and Planning (KICTEP).

References

[1] F.N. Catbas, A.E. Aktan, Condition and damage assessment: issues and some promising indices, ASCE Journal of Structural Engineering 128 (2002) 1026–1036.
[2] J. Kim, J.P. Lynch, Subspace system identification of support excited structures—Part II: gray-box interpretations and damage detection, Earthquake Engineering and Structural Dynamics 41 (2012) 2253–2271.
[3] J. Kim, K. Kim, H. Sohn, In situ measurement of structural mass, stiffness, and damping using a reaction force actuator and a laser Doppler vibrometer, Smart Materials and Structures 22 (2013) 085004.
[4] H.H. Nassifa, M. Gindy, J. Davis, Comparison of laser Doppler vibrometer with contact sensors for monitoring bridge deflection and vibration, NDT & E International 38 (2005) 213–218.
[5] P. Olaszek, Investigation of the dynamic characteristic of bridge structures using a computer vision method, Measurement 25 (1999) 227–236.
[6] M. Celibi, GPS in dynamic monitoring of long-period structures, Soil Dynamics and Earthquake Engineering 126 (2000) 1413–1419.
[7] J. Yang, J.B. Li, G. Lin, A simple approach to intergratio of acceleration data for dynamic soil-strcutrue interaction analysis, Soil Dynamics and Earthquake Engineering 26 (2006) 725–734.
[8] K.T. Park, S.H. Kim, H.S. Park, K.W. Lee, The determination of bridge displacement using measured acceleration, Engineering Structures 27 (2005) 371–378.

[9] M. Gindy, R. Vaccaro, H.A. Nassif, State-space approach for deriving bridge displacement from acceleration, Computer-Aided Civil and Infrastructure Engineering 23 (2008) 281–290.
[10] D.M. Boore, Effect of baseline corrections on displacements and response spectra for several recordings of the 1999 Chi-Chi, Taiwan, earthquake, Bulletin of the Seismological Society of America 91 (2001) 1199–1211.
[11] A. Lawrence, Modern Inertial Technology: Navigation, Guidance, and Control, Springer, New York, NY, 1998.
[12] R.E. Kalman, New results in linear filtering and prediction problems, Journal of Basic Engineering, ASME 82 (1960) 95–108.
[13] A. Smyth, M. Wu, Multi-rate Kalman filtering for the data fusion of displacement and acceleration response measurements in dynamic system monitoring, Mechanical Systems and Signal Processing 21 (2007) 706–723.
[14] C.C. Chang, X.H. Xiao, An integrated visual-inertial technique for structural displacement and velocity measurement, Smart Structures and Systems 6 (2010) 1025–1039.
[15] Z. Li, C.C. Chang, Adaptive noise variance identification for data fusion using subspace-based technique, in: Proceedings of 17th Annual International Symposium on Smart Structures and Materials & Nondestructive Evaluation and Health Monitoring, San Diego, CA, 2010.
[16] D. Simon, Optimal State Estimation, John Wiley & Sons Inc, Hoboken, New Jersey, 2006.